Single Gold Nanowires with Ultrahigh (>10^4) Aspect Ratios by Triphasic Electrodeposition

Guillermo Colón-Quintana[a], Thomas B. Clarke[a], Sakshi A. Ailawar,[a] Jeffrey E. Dick[a,b]*

*jdick@purdue.edu

[a] Department of Chemistry, Purdue University, West Lafayette, IN, 47907, USA

[b] Elmore School of Electrical and Computer Engineering, Purdue University, West Lafayette, IN, 47907, USA

Table Of contents:

Materials and Methods:

Materials:

Fresh solvents were used to prepare each solution immediately before conducting the experiments. Aqueous solutions were made using Millipore GenPure water (18.20 MΩ·cm). Organic solutions were prepared using 1,2-dichloroethane (99% purity) from Sigma-Aldrich (Ward-Hill, MA). The organic salts used in this study, including tetrabutylammonium perchlorate (99% purity), were also obtained from Sigma-Aldrich (St. Louis, MO). Potassium chloride (99% purity) was obtained from Fisher Bioreagents (Fair Lawn, NJ) and was used to prepare all aqueous solutions. Chloroauric acid (99.995% purity) was obtained from Sigma-Aldrich (St. Louis, MO) and was used to prepare all the gold solutions. All the reagents presented and used were of analytical grade and required no additional purification before experimentation.

For the electrochemical experiments here presented indium-tin-oxide glass electrodes (100 mm x 100 mm x 1.1 mm, 7 ohm/sq) were used, these were obtained from Zhuhai Kaivo Optoelectronic Technology Co. (Guangdong, China) and subsequently cut to the desired length and width for experimentation. An Ag|AgCl, 1 M KCl reference electrode, and a glassy carbon counter rod (r = 1 mm) or circular glassy carbon electrode (r = 1.5 mm, used as the counter) were obtained from CH Instruments (Austin, TX) and Thermo Fisher (Tewksbury, MA), respectively. Prior to the experiments, the indium tin oxide glass working electrodes were rinsed thoroughly using Millipore GenPure water (18.20 MΩ·cm) and allowed to dry in the presence of an inert gas to reduce surface impurities and contaminants prior to experimentation. Quartz Theta Tube capillaries (outer diameter 1.2 mm x inner diameter 0.9 mm x length 7.5 mm) were obtained from Sutter instruments (Novato, CA). A salt bridge was employed to connect the reference electrode to the organic solutions to prevent the influence of organic solvents on reference electrode behavior. The salt bridge was created by cooling a 3% agarose (Fischer Bioreagents, Fair Lawn, NJ) solution containing 1 M (Fischer Bioreagents, Fair Lawn, NJ) in a glass tube (99.9%, Sigma-Aldrich, Ward-Hill, MA).

Methods:

The electrochemical experiments presented here were conducted using a standard three-electrode configuration (working electrode, counter electrode, reference electrode) and a CHI 601D potentiostat obtained from CH Instruments (CH Instruments, Austin, TX). Firstly, an organic

solution containing the gold precursor salt ($HAuCl_4$) and the organic alkylammonium salt (tetrabutylammonium perchlorate) was pipetted onto a beaker. Subsequently, an immiscible aqueous solution containing 1M KCl was pipetted on top of the organic solution to allow for the formation of a liquid|liquid interface. The indium-tin oxide working electrode was then carefully submerged, allowing contact with both solutions and forming a three-phase boundary. The glassy carbon rod electrode was then submerged directly into the aqueous top layer (or the glassy carbon commercial macroelectrode was submerged such that the glassy carbon was only contacting the 1,2-dichloroethane phase), and the reference electrode was housed within a separate 1M KCl solution and was connected to the main vial using a salt bridge submerged directly into the aqueous top layer or through the aqueous top layer and into the 1,2-dichloroethane phase.

Optical micrographs were captured using a Leica DMi8 microscope and a 5x (NA 0.12) or 40x objective (NA 0.60) from Leica Microsystems (Germany) and a C15440 OrcaFusionBT sCMOS camera (Hamamatsu, Japan). During brightfield image acquisition, additional light sources were directed at the indium tin oxide where gold nanowires were deposited to increase the amount of scattered light from the wires detected by the camera. This does manifest in different degrees of brightness and contrast of images taken from different nanowires presented in the manuscript. The gold wires were imaged using a scanning electron microscope (SEM) Teneo Volumescope (WSLR S050).

Energy-Dispersive X-Ray (EDX) Spectroscopy Information for The Electrodeposited Gold Nanowires
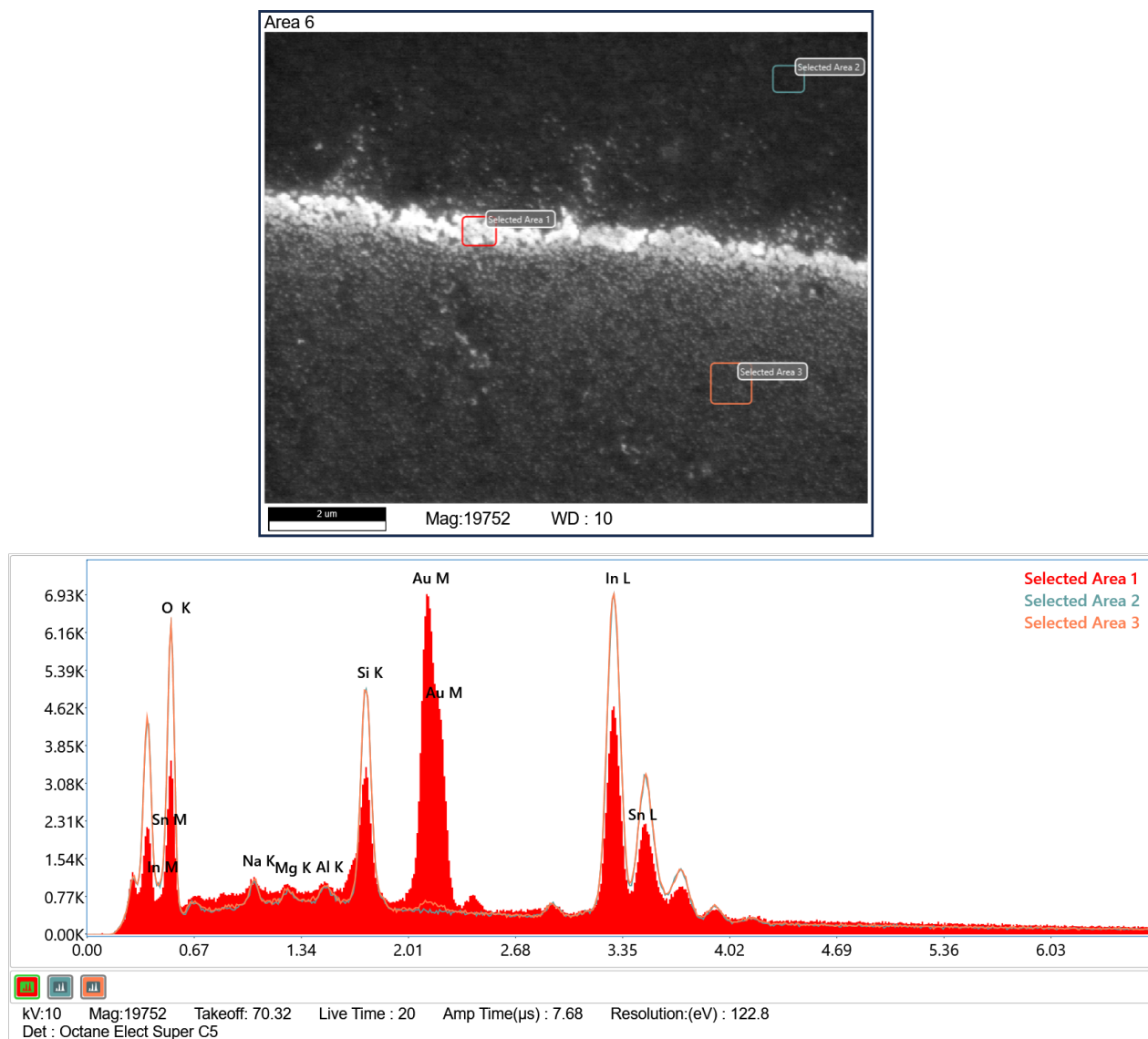

Figure S1: Scanning electron microscopy (SEM) image (top) and energy-dispersive X-ray (EDX) spectra (bottom) taken from the different boxed regions in the SEM image. The red spectrum (Area 1) was taken from the area where the gold was preferentially electrodeposited at the three-phase interface, the blue spectrum (Area 2) was taken from the ITO|water interface, and the orange spectrum (Area 3) was taken from the ITO|DCE interface. This particular deposition was achieved by only applying -0.65 V (vs. Ag|AgCl) for 1 s to the ITO that traversed an interface between 1 M KCl (aq) and 10 mM $HAuCl_4$ + 100 mM $[NBu_4][ClO_4]$ (DCE).

Table S1: Elemental Analysis from EDX Spectrum Shown in Figure S1

Element	Weight %	MDL	Atomic %	Error %	Net Int.
Selected Area 1 – Three-Phase Interface – Analysis Uncertainty: 6.27 %					
O K	5.34	0.14	30.00	9.86	638.67
Na K	0.05	0.08	0.21	68.17	12.13
Al K	0.12	0.09	0.41	40.35	37.00
Si K	3.31	0.1	10.58	5.49	981.33
In L	47.99	0.58	37.54	4.83	2203.40
Sn L	5.24	1.15	3.96	14.25	207.84
Au M	37.94	0.38	17.30	4.39	2724.79
Selected Area 2 – ITO|water – Analysis Uncertainty: 5.69 %					
O K	12.38	0.1	43.27	9.02	1601.63
Na K	1.13	0.07	2.75	9.02	279.89
Mg K	0.70	0.06	1.60	8.27	234.88
Al K	0.87	0.07	1.80	7.40	289.26
Si K	6.21	0.07	12.36	4.52	2046.23
In L	70.59	0.45	34.38	3.70	3745.66
Sn L	8.13	1.2	3.83	10.86	369.34
Selected Area 3 – ITO|DCE – Analysis Uncertainty: 8.10 %					
O K	11.02	0.09	40.37	8.99	1547.92
Na K	1.16	0.07	2.96	8.45	307.95
Mg K	0.85	0.05	2.05	7.08	306.84
Al K	1.11	0.06	2.42	6.84	396.50
Si K	5.78	0.06	12.06	4.48	2037.11
In L	67.22	0.33	34.31	3.55	3820.74
Sn L	10.21	0.99	5.04	6.82	497.39
Au M	2.64	0.22	0.78	5.56	230.90

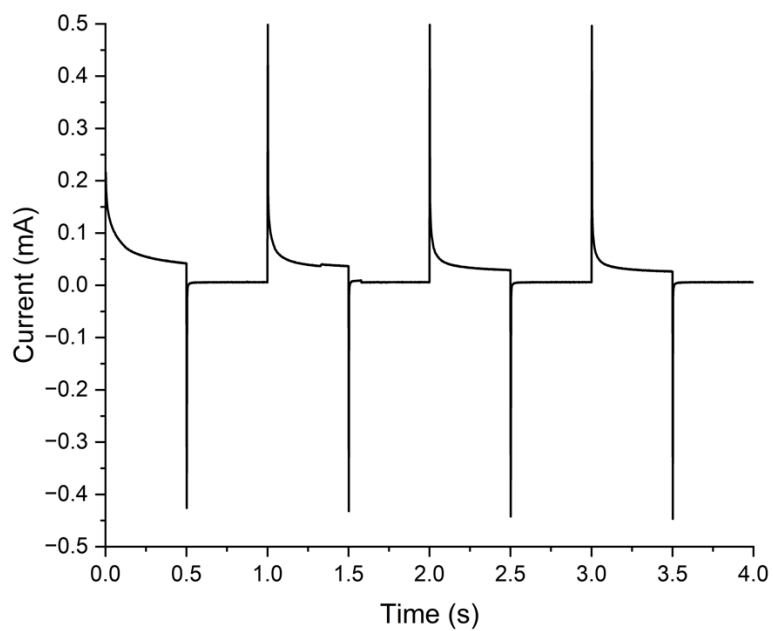Example Current vs. Time Trace for Multi-Potential Step Depositions

Figure S2: Example current vs. time trace for the electrodeposition of gold nanowires on an indium tin oxide (ITO) electrode using 4 cycles of stepping the potential to -0.65 V for 0.5 s and then 0.35 V for 0.5 s. Positive current in this convention corresponds to reducing currents and vice versa.

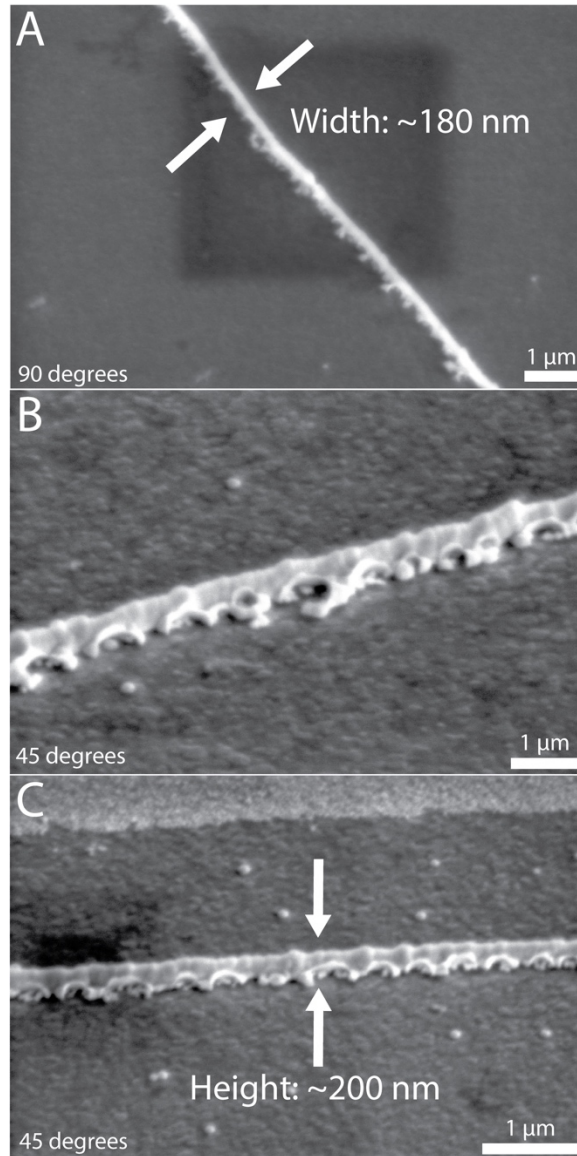Assessing Dimensions of the Nanowires

Figure S3: Scanning electron micrographs of a gold nanowire imaged at A) 90° relative to the indium tin oxide (ITO) electrode surface and B-C) 45° relative to the ITO surface. The measured width at the marked location in (A) was ~ 180 nm, while the measured height at the marked location in (C) was ~ 200 nm, indicating that the deposited nanowires can be quite hemicylindrical.
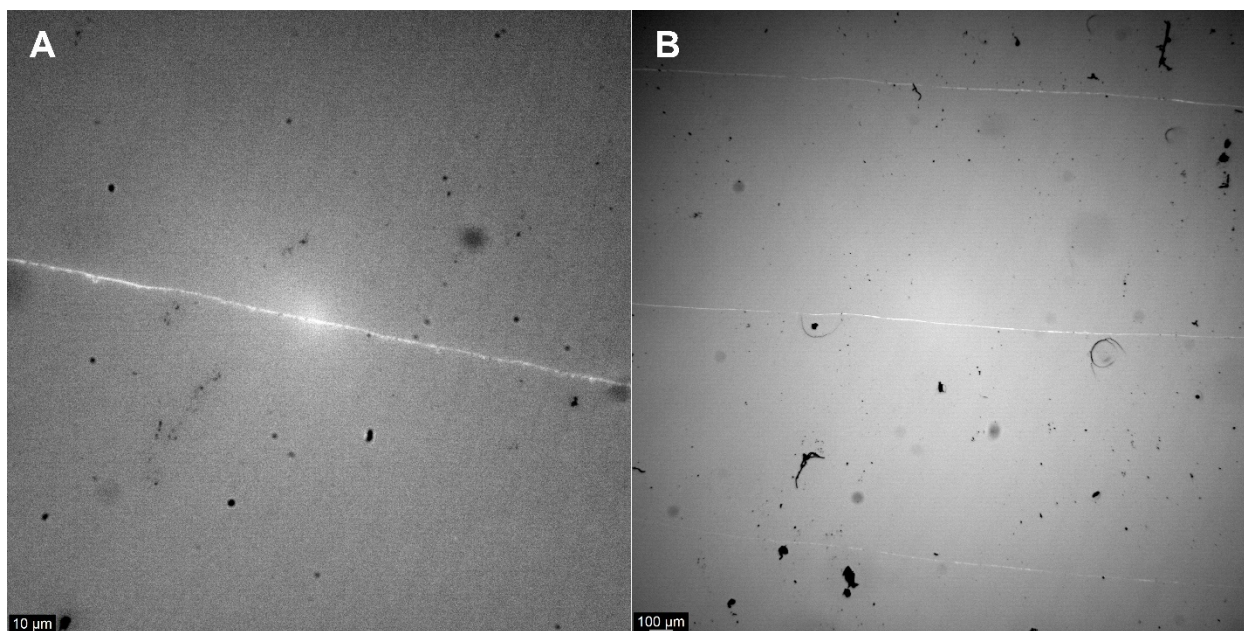
Figure S4: Tunable deposition of multiple nanowires. Changes in the ITO working electrode position were used to deposit multiple nanowires on a single electrode surface. A multipotential step chronoamperometric method was used for all the experiments shown here; the repetition of cycles consisted of quick potential shifts between –0.65 V vs. Ag|AgCl for 0.5 s, followed by 0.3 V vs. Ag|AgCl for 0.5 s for 2 cycles. Images A) and B) show light microscopy images of gold nanowires on our ITO surface, with B) showing 3 gold nanowires and A) being an increased magnification focused on the central wire.

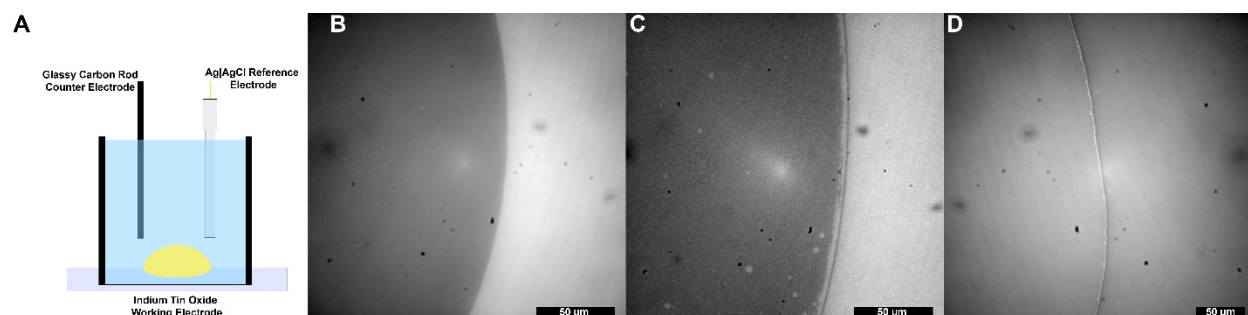Light microscopy images of gold nanowires electrodeposition under different geometries

Figure S5: Light microscopy images of gold nanowires electrodeposition under different geometries. Where A) shows a schematic representation of the system under study for a two-phase system where a 10 mM $HAuCl_4$ in 1,2-dichloroethane (DCE) solution containing 100 mM tetrabutylammonium perchlorate ($[NBu_4][ClO_4]$) droplet is pipetted on to the surface of ITO and surrounded by an aqueous solution containing 1 M KCl. A standard three-electrode system can be seen, consisting of an ITO working electrode, a glassy carbon rod counter electrode (r = 1 mm), and an Ag|AgCl (1 M KCl) reference electrode. Images B) and C) correspond to light microscopy images before B) and after C) the electrodeposition of gold wires. Image D) corresponds to light microscopy images after the droplet on the surface was removed post-deposition to allow for observation and imaging. Observed circular inclusions did not yield observable gold deposition post-deposition via scanning electron microscopy imaging or optical microscopy, suggesting the presence of a bubble or entrapped solvent.

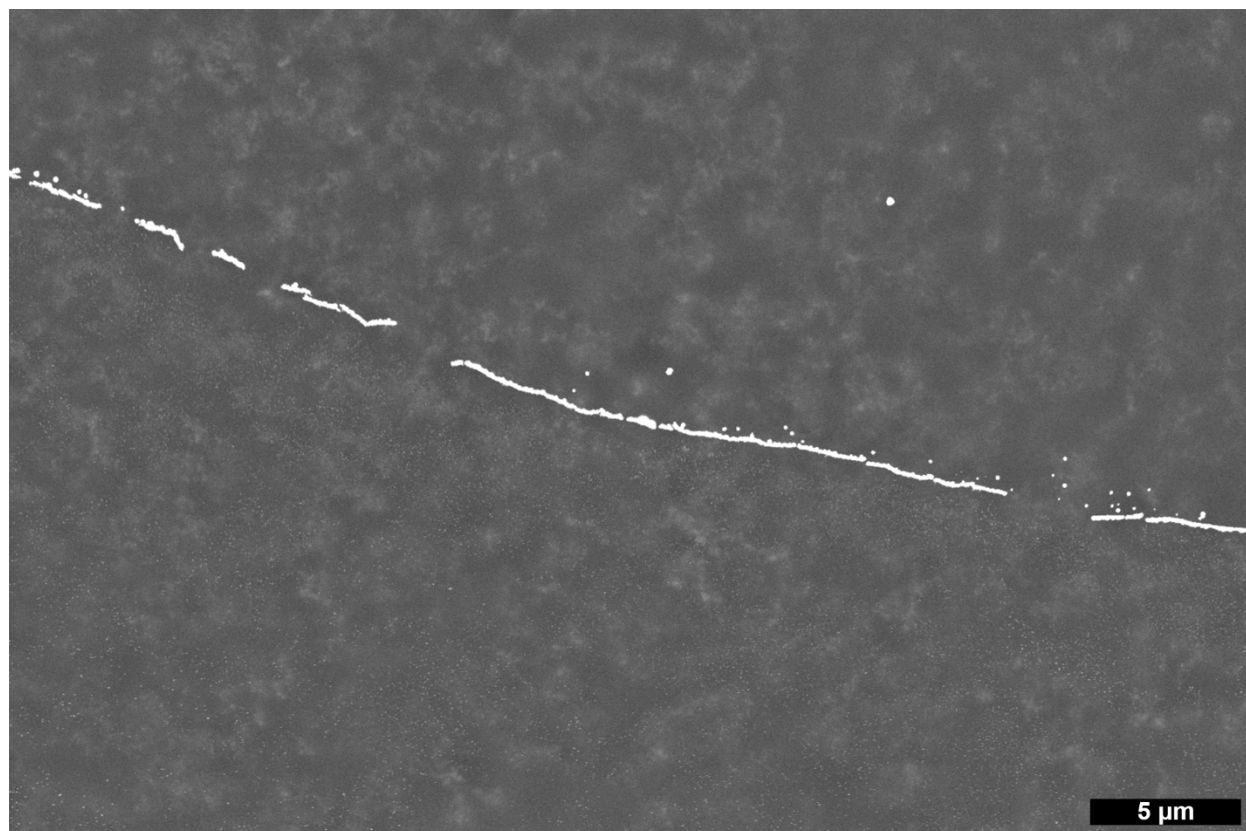Scanning Electron Microscopy Image of an Exfoliated Gold Nanowire

Figure S6: Scanning electron microscopy image of exfoliated gold nanowire on carbon tape post-electrodeposition. A multipotential step chronoamperometric method was used; the depositional cycle consisted of quick potential shifts between –0.65 V vs. Ag|AgCl for 0.5 s, followed by 0.3 V vs. Ag|AgCl for 0.5 s. After deposition, a strip of carbon tape was placed on top of the sample, used to exfoliate nanowires off the electrode surface, and subsequently imaged.
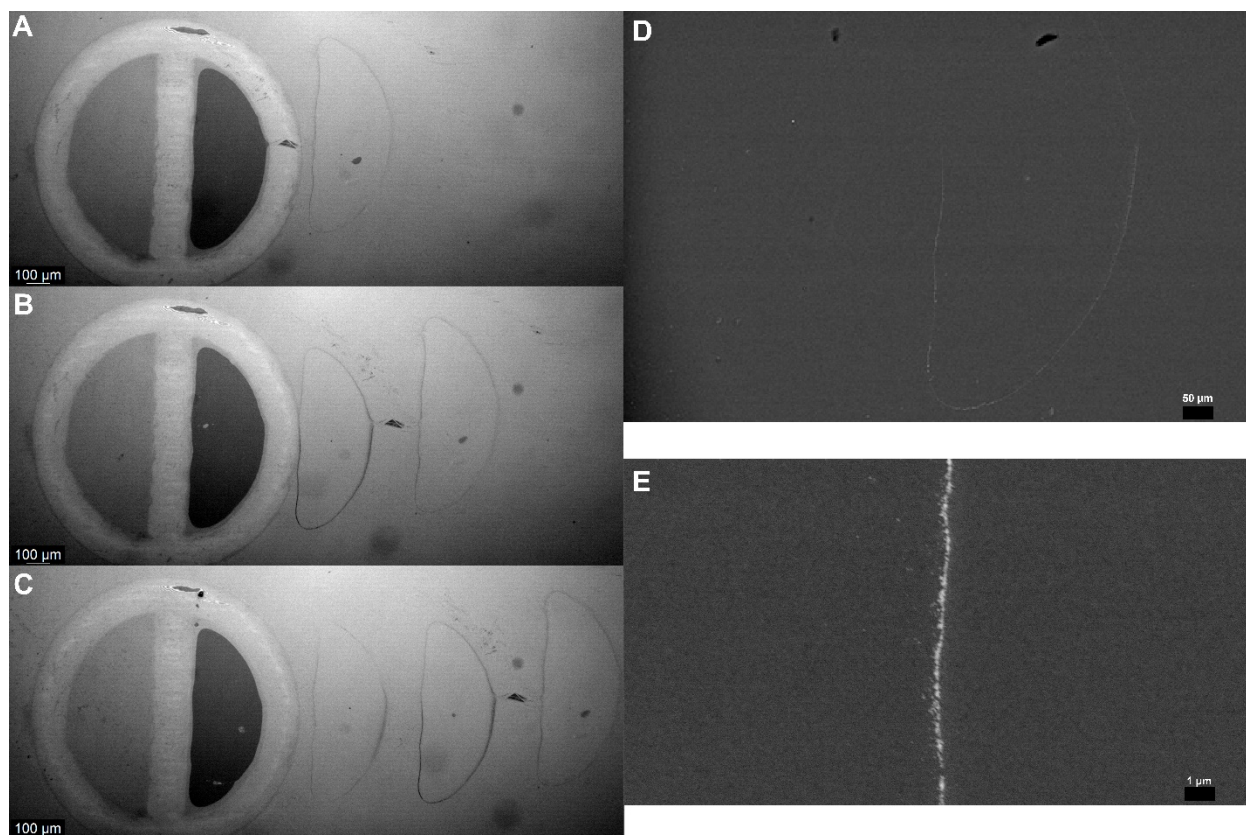
Figure S7: Tunable shape deposition of nanowires. A capillary theta was used to change droplet geometry and deposit multiple "D" shaped nanowires on a single electrode surface. The capillary was lightly pressed on to our conductive surface and subsequently filled with a 0.1 M tetrabutylammonium perchlorate ($[NBu_4][ClO_4]$) and 10mM chloroauric acid 1,2-dichloroethane solution. A multipotential step chronoamperometric method was used for all the experiments shown here; the repetition of cycles consisted of quick potential shifts between –0.65 V vs. Ag|AgCl for 0.5 s, followed by 0.3 V vs. Ag|AgCl for 0.5 s for 2 cycles. Images A) to C) show light microscopy images of gold wires deposited on our ITO surface, with A) showing images after a single deposition, and B) to C) showing an increasing number of "D" shaped depositions. Image D) shows the same nanowire shown in A) under scanning electrochemical microscopy. Image E) shows an increase in magnification for the wire shown in D).
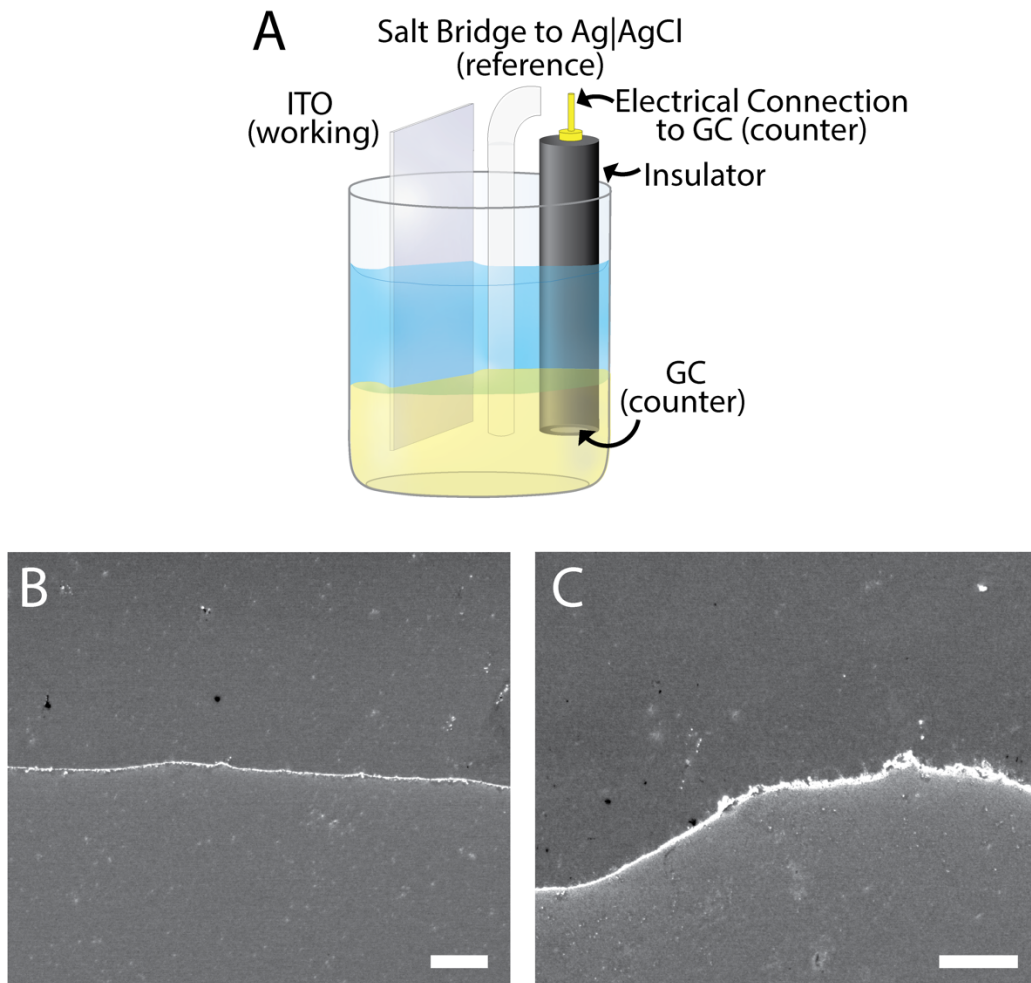
Figure S8: A) Schematic of experimental setup for the control experiment where the counter electrode surface is only contacting the bottom, 1,2-dichloroethane phase, which contains 10 mM chloroauric acid and 100 mM tetrabutylammonium perchlorate. Here, a glassy carbon rod electrode is replaced with a commercial glassy carbon (GC) electrode (d = 3 mm) encased in an insulating material, where the GC surface is only contacting the dichloroethane phase. An indium tin oxide (ITO) working electrode traverses both the aqueous phase (containing 1 M KCl) and the 1,2-dichloroethane phase. Additionally, a salt bridge connects the 1,2-dichloroethane to a a Ag|AgCl electrode (1 M KCl). Amperometry was conducted where -0.65 V vs. the Ag|AgCl reference was applied at the ITO working electrode for 1 s. B) and C) scanning electron micrographs from different regions of the same nanowire showing that preferential electrodeposition of gold still occurs along the water|1,2-dichloroethane|indium tin oxide (ITO) interface. Scale bars represent 10 μm.

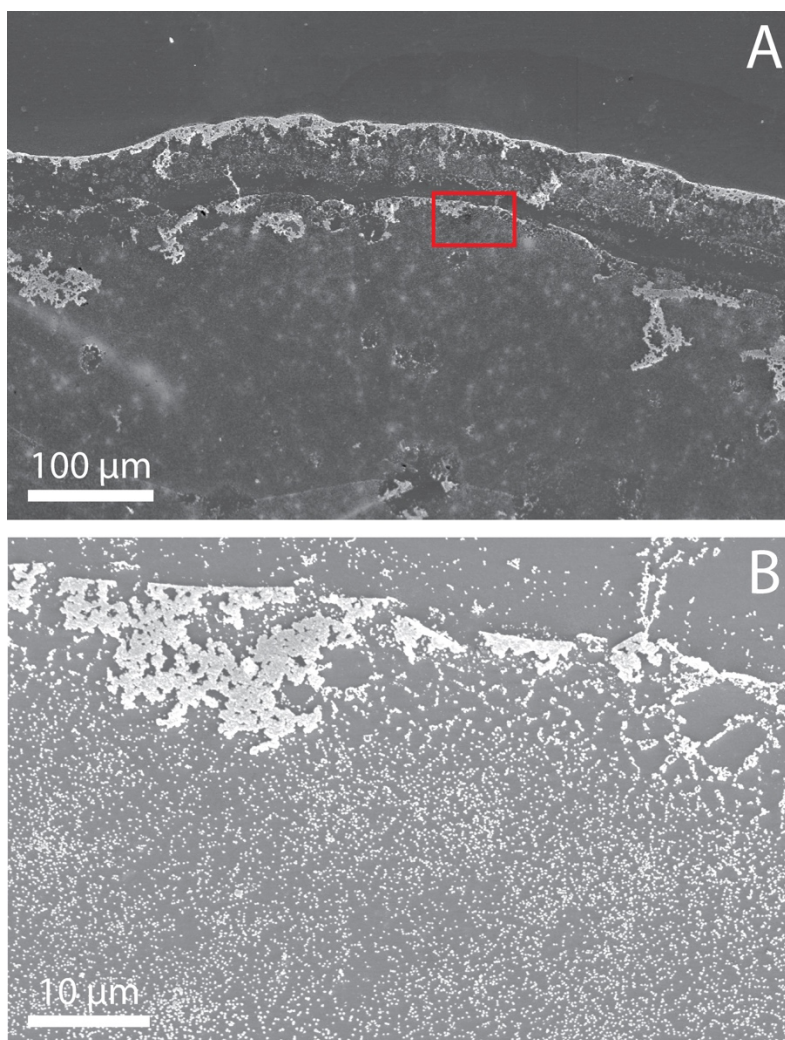Nanowires and Nanoparticles Deposted at a Larger Overpotential

Figure S9: Scanning electron micrographs of an indium tin oxide (ITO) working electrode was used in the Figure 1 experimental setup from the main text, except -0.9 V was applied to the ITO for 1 s. Micrograph A) was taken at a lower magnification and micrograph B) was taken at a higher magnification from the region highlighted by a red box in (A). Electrodeposition of gold still occurs preferentially along the water|1,2-dichloroethane|ITO interface, but gold nanoparticles are still observed below this region, corresponding to the region where the ITO interfaced with the dichloroethane phase, which contained 10 mM $HAuCl_4$ and 100 mM $[NBu_4][ClO_4]$.